

Algorithm Theoretical Basis Document

GCOM-C Evapotranspiration Index Product

Version 1.4

Masahiro Tasumi

Department of Forest and Environmental Sciences, University of Miyazaki

March 28, 2021

Abstract

This Algorithm Theoretical Basis Document (ATBD) describes the algorithm for estimating Evapotranspiration Index (ET_{index}) developed as a research product of the GCOM-C satellite of the Japan Aerospace Exploration Agency (JAXA). The ET_{index} expresses actual evapotranspiration normalized for the weather condition and is equivalent to the crop coefficient, which has been applied widely for agricultural and irrigation water management around the globe. The ET_{index} is convertible to the actual quantity of evapotranspiration by using a local or global weather dataset. The ET_{index} is estimated primarily by GCOM-C land surface temperature observation, with some additional inputs including those of a Digital Elevation Model (DEM) and global wind speed data. The final product is a cloud-free 16-day global ET_{index} map having a spatial resolution of 250 m. Daily actual evapotranspiration for any weather condition (including cloud-cover days) is further estimable using a ground-based weather dataset. Additionally, the ET_{index} is convertible to volumetric soil water content for locations where information of soil physical characteristics is available.

Employing two extreme hypothetical surface conditions named “wet surface,” defined as a surface having zero sensible heat flux, and “dry surface,” defined as a surface having zero ET, the algorithm estimates ET_{index} by using surface temperature as an indicator of surface wetness. The algorithm described in this ATBD has been applied with the MODIS daily land surface temperature map and a global weather dataset. The estimated result was compared with other independent global ET datasets and with some other environmental properties. The comparison implied that the proposed algorithm reasonably estimates ET_{index}.

Table of Contents

1. Introduction.....	1
2. GCOM-C Evapotranspiration Index Estimation Procedure—Overview and Definitions	2
2-1. GCOM-C Evapotranspiration Index Map	2
2-2. Application of GCOM-C ETindex Product to Soil Moisture Estimation	7
3. Algorithm Descriptions.....	8
3-1. Basic Strategy for Estimating Ts(wet) and Ts(dry)	8
3-2. Data for Analyses	9
3-3. Ts(wet) Estimation.....	11
3-4. Ts(dry) Estimation	18
3-5. Calibration for the Maximum Limit of ETindex.....	23
3-6. Adjustments and Filtering of ETindex Values on Daily Computation.....	24
3-7. ETindex Composite	27
3-8. Extra Adjustment of ETindex Values by Applying Soil Water Balance Model (Optional - Recommended)	28
3-9. Calculation of Soil Moisture (Optional).....	29
4. Application to Satellite Imagery and Information about Model Accuracy	30
4.1. Global Application Test using MODIS Land Surface Temperature Product ...	30
4.2. Regional Application Test using GCOM-C Land Surface Temperature Product	32
4.3. Analysis of ETindex for Model Applicability	33
4.4. Reality Check of the Estimated Values using Outside Sources.....	34
Acknowledgements	37
References.....	38
Appendix: Ts(wet) and Ts(dry) determination model for Shenmu weather measurement site.....	1

1. Introduction

Surface evapotranspiration (ET) and near-surface soil moisture are important factors in climate, water balance and circulation, and crop production. The need for satellite-based, global ET estimation has been increasing with the growth of large-scale water and environmental issues, such as global warming, increased instability of weather and climate, water shortages due to population growth, and enhanced human activities. Under these circumstances, the estimation algorithm of the global Evapotranspiration Index (ET_{index}) has been investigated as one of the GCOM-C research products. The ET_{index} is valuable as an index of evapotranspiration efficiency and soil moisture content. The index is also convertible to the actual amount of ET from the land surface by using a global or local near-surface general weather dataset.

Because the ET_{index} is closely related to soil water availability, the information is further convertible to volumetric soil water content (θ), with some additional information of soil physical characteristics, especially that pertaining to the water holding characteristic of soil. Although soil moisture estimation is not the main target of our study for the ET_{index} product, this Algorithm Theoretical Basis Document (ATBD) describes the progress toward soil moisture estimation found during the algorithm development work of the ET_{index} product.

The first ATBD (version 1.0) was submitted to JAXA in September 2011. The major update from ATBD ver. 1.0 to ver. 1.1 (submitted in March 2013) was the elimination of the elevation function in the estimation of wet-surface temperature. The latitude function was also corrected and modified. The update from ATBD ver. 1.1 to ver. 1.2 (submitted in October 2014) included modification of the ET_{index} regulation method and correction of the equations. The update from ATBD ver. 1.2 to ver. 1.3 (submitted in March 2016) updates the theoretical background information includes the product accuracy. The development of the ET_{index} estimation algorithm is an on-going project. The detailed procedures for ET_{index} estimation will continue to be improved, and the ATBD will be updated as necessary.

2. GCOM-C Evapotranspiration Index Estimation Procedure—Overview and Definitions

2-1. GCOM-C Evapotranspiration Index Map

Evapotranspiration (ET) is controlled by energy and soil water availability along with the near-surface heat and vapor exchange circumstances. The quantity of ET is affected by several factors including weather related factors such as solar radiation, surface and air temperatures, humidity, and wind speed and precipitation, as well as surface topography, land cover, soil type, and status of vegetation. Many of these factors are strongly dependent on region and time, which makes automated global estimation of ET technically difficult. To develop the information infrastructure of global water circulation and consumption, by minimizing the technical difficulty caused by the dependency on region and time, we suggest providing global ET_{index} via GCOM-C earth observation. The ET_{index} is ET normalized for the weather condition. The technical difficulty of global ET estimation is mitigated effectively by this normalization.

The GCOM-C ET_{index} is equivalent to the crop coefficient, which has been applied widely for agricultural and irrigation water management around the globe. The ET_{index} is defined by the following equation:

$$ET_{index} = \frac{ET_{act}}{ET_0} \quad (1)$$

where ET_0 is reference ET and ET_{act} is actual ET.

ET_0 is typically described as the ET from a well-watered, 12-cm tall grassy field. A detailed definition of ET_0 is the ET from a hypothetical grassy reference field with a crop height of 12 cm, surface resistance of 70 s/m, and albedo of 0.23. ET_0 is calculated using only near-surface weather data (solar radiation, air temperature, humidity, and wind speed). The calculation procedure of ET_0 is described in Allen et al. (1998).

Using the ET_{index} map and a weather dataset, users can back-calculate actual ET as

$$ET_{act} = ET_{index} \times ET_0 \quad (2)$$

Framework of the GCOM-C ET_{index} Algorithm

In order to achieve a global and near-timely estimation of daily ET_{index} with a spatial resolution of 250 m, the algorithm should be as simple as possible, with a minimum requirement of input data. In this algorithm, the input data that are used for ET_{index} computation are limited to GCOM-C observation data, global DEM data, and near-surface wind speed data.

Our model adopts, from among several types of ET estimation approaches, an estimation approach that produces an index of surface temperature. Kogan (1995) suggested that a surface temperature index having the form of Eq. 3, named the temperature condition index (TCI), can adequately express drought-related vegetation stress:

$$TCI = \frac{Ts(max) - Ts(act)'}{Ts(max) - Ts(min)} \quad (3)$$

where Ts(max) and Ts(min) are the multi-year weekly maximum and minimum surface temperatures, respectively, and Ts(act)' is weekly actual surface temperature (°C).

Kimura (2007) and Senay et al. (2007) proposed indices named the modified temperature/vegetation dryness index (MTV_{DI}) and the ET fraction (ET_f), respectively. These indices estimate surface evapotranspirative efficiency using the basic structure of a temperature index, as does the TCI, but the timescales of the actual, maximum, and minimum temperatures are instantaneous rather than weekly or multi-annual. In our model, following their findings, the ET_{index} is estimated as

$$ET_{index} = C_{adj} \times \frac{Ts(dry) - Ts(act)}{Ts(dry) - Ts(wet)} \quad (4)$$

where Ts(act) is the instantaneous actual surface temperature from satellite thermal

observation ($^{\circ}\text{C}$) and $T_s(\text{wet})$ and $T_s(\text{dry})$ are the hypothetical wet surface temperature and the dry surface temperature ($^{\circ}\text{C}$), which are the instantaneous surface temperatures when the surface is expected to have zero sensible heat flux and when the surface is expected to have zero latent heat flux, respectively. The constant C_{adj} is an adjustment factor employed in the algorithm.

The constant C_{adj} in the equation, representing the maximum limit of the ET_{index} occurring when the surface is in a very wet condition, is uniquely employed in the GCOM-C ET_{index} algorithm. Figure 1 shows an overview of the algorithm for ET_{index} estimation.

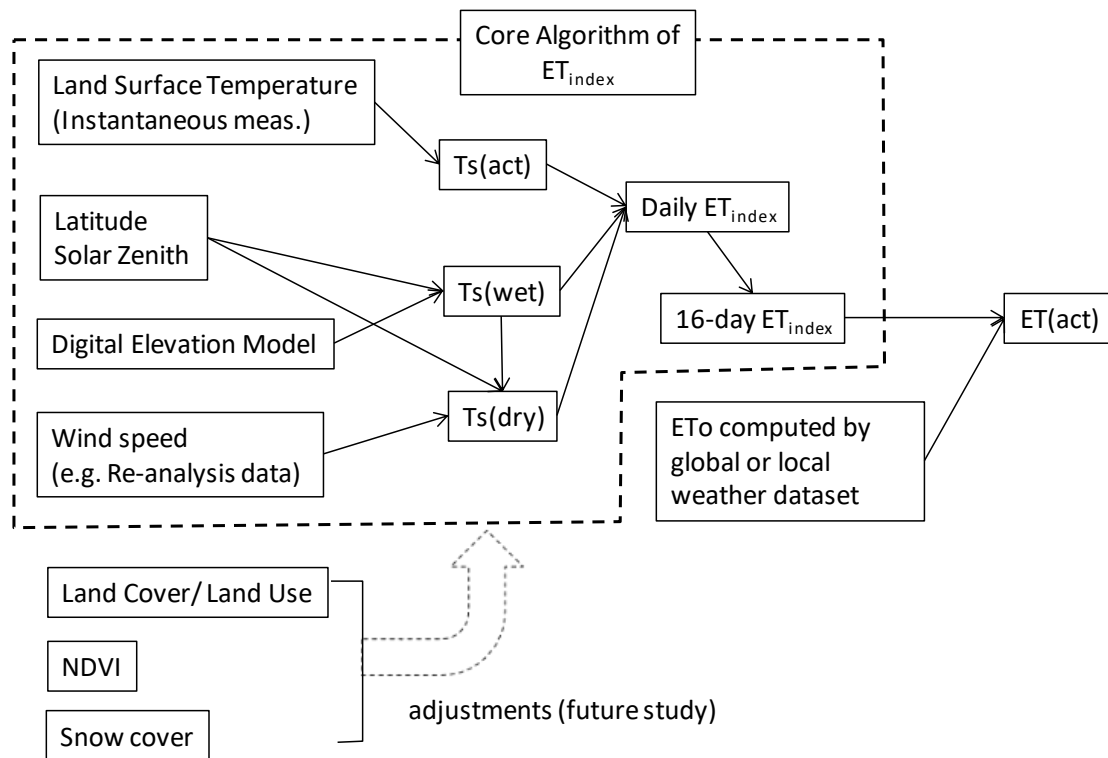


Figure 1. Flowchart of the GCOM-C ET_{index} estimation algorithm.

Calculation Time Interval

The ET_{index} is first processed on a daily basis, for every day, including cloudy days, using daytime instantaneous land surface temperature (LST) images. The direct estimation of ET_{index} is applicable only for the moment when actual surface temperature is observed by the GCOM-C satellite. For extension of the estimation to a 24-hour

period, we employ an assumption, similar to that of Allen et al. (2007), that the instantaneous ET_{index} computed at image time is the same as the 24-hour average ET_{index} . GCOM-C will observe the surface every day or two. However, the presence of clouds critically degrades or disables surface temperature observation and thus ET_{index} estimation. A small contamination by clouds in a pixel cell, which may be undetectable by an automated cloud-mask algorithm, can cause significant overestimation of ET_{index} due to a reduction in the retrieved $T_s(\text{act})$ value. To automatically prevent the impact of cloud contamination in global ET_{index} estimation, daily estimated ET_{index} maps are composited every 16 days, and the minimum value of ET_{index} over the 16-day period is selected for each pixel as the representative ET_{index} value of the 16-day period. However, in some extreme climatic conditions, no single clear-sky day is available within a 16-day composite period. In such cases, because of the cloud effect, the pixel value of the ET_{index} automatically takes the maximum number, which may be a good approximation because more than 16 days of continuous cloud is an indicator of the rainy season, during which the surface is expected to be in a wet condition and the ET_{index} is expected to take a large number. We accept this assumption for the following reasons:

- (1) Such a condition is expected only in limited areas/seasons of the world.
- (2) Such a condition typically occurs during the rainy season, when the land surface beneath the clouds is in a wet condition and the actual ET_{index} value is likely not far from the maximum.
- (3) We want to avoid any data-lacking pixels. Supplying a complete set of 16-day ET_{index} maps, with no data-lacking pixels anywhere, is a big advantage. For example, annual ET cannot be estimated if a period lacking data is included.
- (4) In such a cloudy condition with weak solar radiation, ET is expected to be small. Thus, the error in ET is expected to be small even if a somewhat larger error is present in the ET_{index} .

Application of the Output Data

The GCOM-C ET_{index} is applicable to the following purposes:

- (1) Estimate actual ET from GCOM-C ET_{index} and weather data.
Users can derive daily, monthly, and annual actual ET maps from the ET_{index} map by applying a global or local weather dataset. The required weather data are typically obtainable from any major global weather dataset source or from public

weather stations within or near the users' area of interest.

- (2) Use the GCOM-C ET_{index} map for relative analyses.

The ET_{index} map is a relative indicator of ET. In a specific ET_{index} image of an area, pixels having higher ET_{index} have higher actual ET. Therefore, the map is usable as is for relative analyses, e.g., identifying areas having higher/lower ET or understanding the yearly trend of ET.

2-2. Application of GCOM-C ET_{index} Product to Soil Moisture Estimation

The GCOM-C ET_{index} essentially indicates the level of soil wetness from zero (very dry) to the maximum (very wet), and it is valuable for estimating soil moisture. The additional input data required to estimate soil moisture are the water holding characteristic of the soil (typically estimated by soil type if directly measured information is not available) and the average root zone depth of the vegetation (if vegetation is present over the surface).

The volumetric soil water content (θ) for the average depth at which the soil water significantly contributes to surface ET can be estimated from the ET_{index}. The depth is represented as the root zone if the surface is covered by vegetation or by the top 10–15 cm if the surface is in a bare-soil condition. The volumetric soil water content (m^3/m^3) is defined by the following equation:

$$\theta = (\text{Volume of soil water})/(\text{Total volume of soil}) \quad (5)$$

Additional and more-detailed information about the soil water estimation procedure using GCOM-C ET_{index} is available in Tasumi and Kimura (2013).

3. Algorithm Descriptions

Estimation of wet surface temperature ($T_s(\text{wet})$) and dry surface temperature ($T_s(\text{dry})$) is key to the estimation of ET_{index} , as shown in Equation 4 and in Figure 1. This section describes the computational algorithms of $T_s(\text{wet})$ and $T_s(\text{dry})$.

3-1. Basic Strategy for Estimating $T_s(\text{wet})$ and $T_s(\text{dry})$

The GCOM-C ET_{index} is estimated by indexing surface temperature, which requires two hypothetical surface temperatures, the wet surface temperature ($T_s(\text{wet})$) and the dry surface temperature ($T_s(\text{dry})$). $T_s(\text{wet})$ is the hypothetical surface temperature assuming that the surface is in a very wet condition. The “wet” surface is defined here as the surface having latent heat equivalent to available energy (i.e., sensible heat is zero). $T_s(\text{dry})$ is the hypothetical surface temperature assuming that the surface is in a very dry condition. The “dry” surface is defined here as the surface having zero latent heat flux (i.e., zero ET). The definitions of the two extreme surfaces are equivalent to the “cold pixel” and the “hot pixel” of the SEBAL ET estimation algorithm of Bastiaanssen et al. (1998). Whereas the cold and hot pixels of SEBAL are specific pixels of an image, the $T_s(\text{wet})$ and $T_s(\text{dry})$ of the GCOM-C ET_{index} algorithm are not temperatures of specific pixels but temperatures assigned for every pixel individually.

Theoretically, $T_s(\text{wet})$ and $T_s(\text{dry})$ can be determined by solving surface radiation and heat balance (i.e., energy balance) by employing specific assumptions for wet and dry surfaces. However, we have found operational difficulty in obtaining the theoretical solutions of $T_s(\text{wet})$ and $T_s(\text{dry})$. The theoretical approach determines $T_s(\text{wet})$ and $T_s(\text{dry})$ by solving energy balance equations to derive long-wave radiation from earth to sky (L_{out}) and then converts L_{out} to the hypothetical temperatures. The structural problem of this procedure is that all uncertainties and errors in energy balance computation are cumulated and passed to $T_s(\text{wet})$ and $T_s(\text{dry})$. Therefore, input data quality and robust definition of the hypothetical surface characteristics are critical for successful estimation of the hypothetical temperatures. Because we cannot satisfy these requirements of input data quality and robust definitions of the surface characteristics, using the theoretical approach is operationally difficult. Instead, the GCOM-C ET_{index} algorithm takes an empirical approach to determine $T_s(\text{wet})$ and $T_s(\text{dry})$.

3-2. Data for Analyses

The development of empirical equations for $T_s(\text{wet})$ and $T_s(\text{dry})$ requires near-surface radiation and heat balance measurements. The current version of the algorithm relies largely on micrometeorological data, supplied by Dr. Kimura of Tottori University, measured at Shenmu, China, during 2005 to 2008. The site is located in a part of the Loess Plateau, in a semiarid region of China. Photographs of the weather station and the surrounding area are shown in Figure 2. The data include air temperature, humidity, wind speed and direction, four separated radiation components (solar radiation, reflectance, and longwave radiations from earth and from sky), and soil moisture for 10 different depths. The details of the data measurement are described in Kimura (2007).

Using the weather data, $T_s(\text{wet})$ and $T_s(\text{dry})$ were computed by an energy balance model described in the Appendix of this document. An example calculation result for September 9, 2005, is shown in Figure 3.



Figure 2. Photographs of weather station (left) and surrounding area (right) of the Shenmu measurement site ($38^{\circ}47'$ N, $110^{\circ}21'$ E; 1224 m a.s.l.).

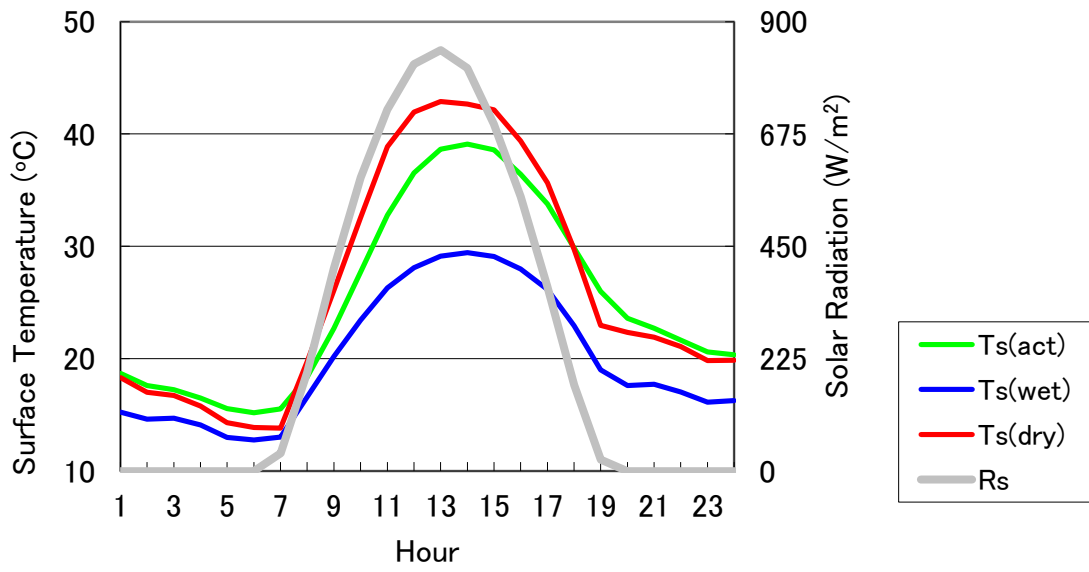


Figure 3. Ts(wet) and Ts(dry) estimated by energy balance computation, plotted with measured actual Ts and Rs at Shenmu, for 9/9/2005.

3-3. Ts(wet) Estimation

Wet and dry surface temperatures at 10:30 A.M. on clear-sky days tend to have a linear relationship with radiation, such as solar radiation (R_s) or net radiation (R_n) (Tasumi, 2010, 2011). Thus, $T_s(\text{wet})$ and $T_s(\text{dry})$ are estimated using R_s or R_n . Considering the theoretical energy and temperature relationship, R_n is a more appropriate term to use than R_s , because R_s is only one part of the surface radiation balance. Nevertheless, we suggest adopting R_s to estimate $T_s(\text{wet})$ and $T_s(\text{dry})$ because using R_n results in some operational problems that are difficult to solve.

Considering the global application of the algorithm with GCOM-C satellite measurements, estimating R_s is much easier than estimating R_n , because the evaluation of longwave radiation from sky to land surface is difficult. Moreover, the critical problem of using R_n for $T_s(\text{wet})$ and $T_s(\text{dry})$ estimations is the difference between R_n over an actual surface and R_n over the hypothetical wet and dry surfaces. R_n over the hypothetical surfaces is the appropriate term to use to estimate $T_s(\text{wet})$ and $T_s(\text{dry})$. However, R_n cannot be determined without knowing the hypothetical surface temperatures. Thus, we cannot use R_n over the hypothetical surfaces for the estimations of hypothetical temperatures. On the other hand, the solar radiation of the hypothetical surfaces is the same as the actual solar radiation. Thus, we can operationally use R_s for hypothetical surfaces without any problem.

A problem related to the application of actual (not hypothetical) R_n to estimate $T_s(\text{wet})$ and $T_s(\text{dry})$ is visualized in Figure 4. For a certain small area at 10:30 A.M., the spatial difference of net radiation depends on surface temperature and albedo. Hot and bright desert has much lower net radiation than cold forest. If $T_s(\text{wet})$ is estimated by actual R_n using an empirical linear regression equation, the estimated $T_s(\text{wet})$ of desert will be much lower in desert than in forest, which is probably not realistic. If the hot and bright desert is in a very wet condition, R_n of the surface should be very similar to R_n of the cold forest, and the $T_s(\text{wet})$ estimation of the area will be much more homogeneous. This problem is avoided if we use R_s as the independent variable to estimate the hypothetical surface temperatures.

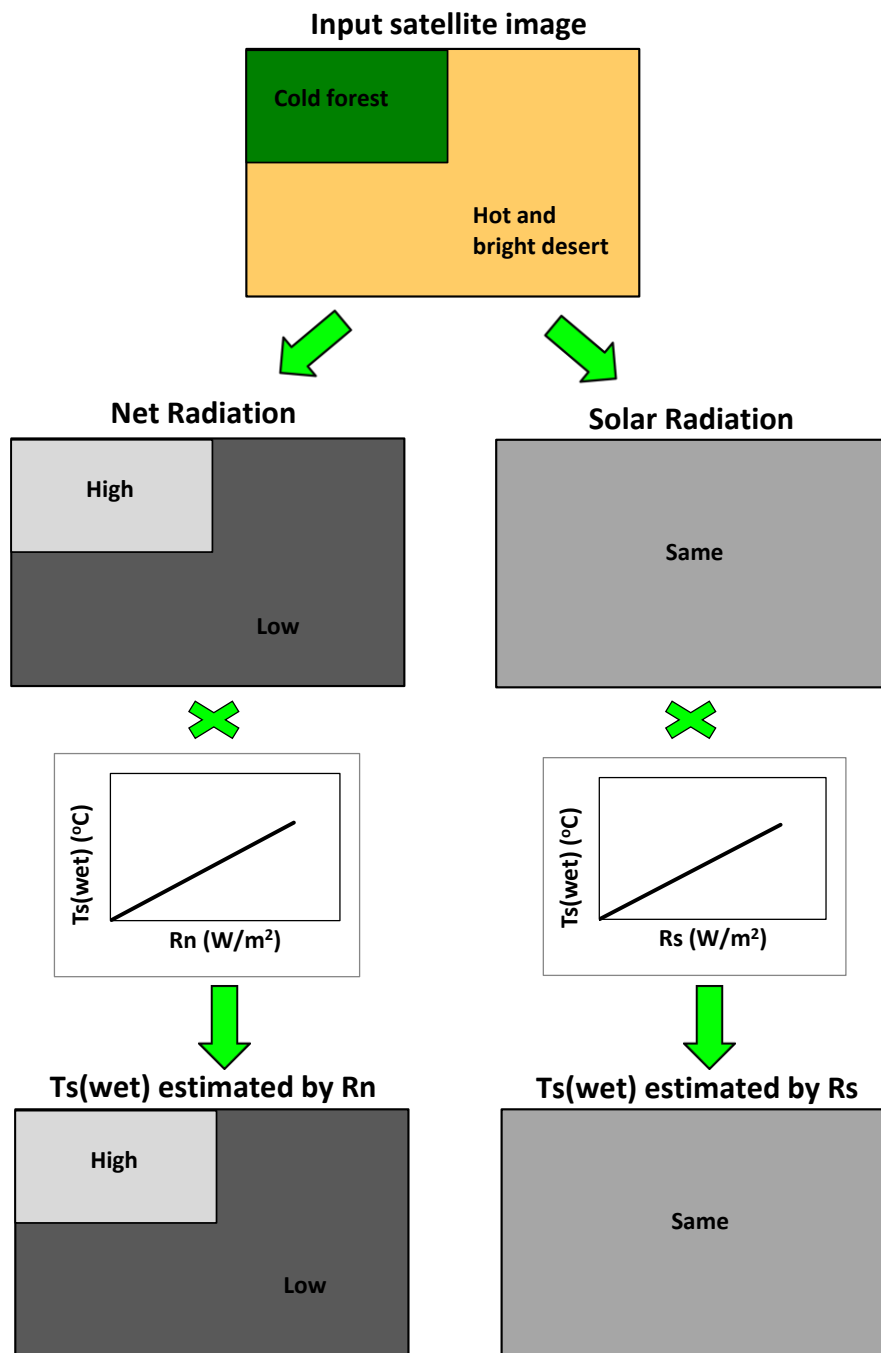


Figure 4. Expected result of $T_s(\text{wet})$ estimated by net radiation and by solar radiation.

Figure 5 shows the relationship between solar radiation and $T_s(\text{wet})$ at Shenmu, China, at about 10:30 A.M. (solar time) for clear-sky days during 2005-2008. A clear linear relationship, with large scatter, between R_s and $T_s(\text{wet})$ is confirmed. If $T_s(\text{wet})$ is estimated by the linear regression equation shown in the figure, the standard error of estimation is 7.83 °C, which is large.

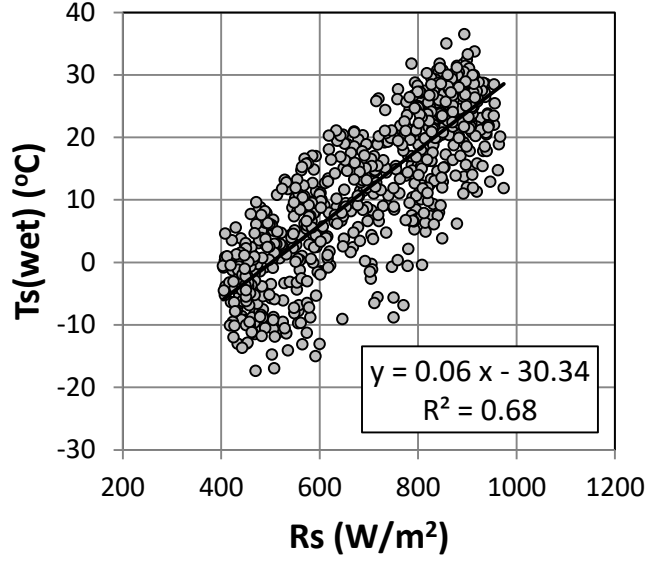


Figure 5. Relationship between measured solar radiation and estimated $T_s(\text{wet})$ at Shenmu, China, at about 10:30 A.M. (solar time) for clear-sky days during 2005-2008.

The primary reason for the large scatter in Figure 5 is seasonal differences caused by the thermal inertia of the Earth. Figure 6 uses exactly the same data used in Figure 5, but shown as monthly averages. A clear seasonal trend of R_s and $T_s(\text{wet})$ is shown, and the trend can be explained theoretically by the thermal inertia of the Earth. In this version of ATBD, the R_s vs $T_s(\text{wet})$ relationship with the seasonal trend was expressed as the following equation:

$$T_s(\text{wet}) = 0.06R_s - 30.34 - \sin\left(\frac{\text{DoY} + S_{\text{day}}}{365} \times 2\pi\right) \times f(\text{Lat}) - C_{\text{top}} \times (z_p - z_b) \quad (6)$$

where $T_s(\text{wet})$ is in °C, R_s is in W/m^2 , DoY is day of year, S_{day} is the phase shift of the sine curve calibrated as 37 in the Northern Hemisphere and 220 in the Southern Hemisphere, z is elevation in meters, and $f(\text{Lat})$ is the amplitude of the sine curve

determined using latitude (deg.) by $f(\text{lat}) = -0.0021 \cdot \text{Lat}^2 + 0.3449 \cdot |\text{Lat}| - 2.9864$ ($0.0 \leq f(\text{lat}) \leq 10.0$), C_{top} is a coefficient for the topographic adjustment that is tentatively calibrated as 0.0098 ($^{\circ}\text{C}/\text{m}$), which is equivalent to dry-adiabatic lapse rate, z_p is the elevation of the pixel (m), and z_b is the lowest elevation of the surrounding 15 km by 15 km area (m), where the pixel is at the center of the 15 km by 15 km area. The z_p and z_b are intended to be derived using a 250 m resolution digital elevation model (DEM).

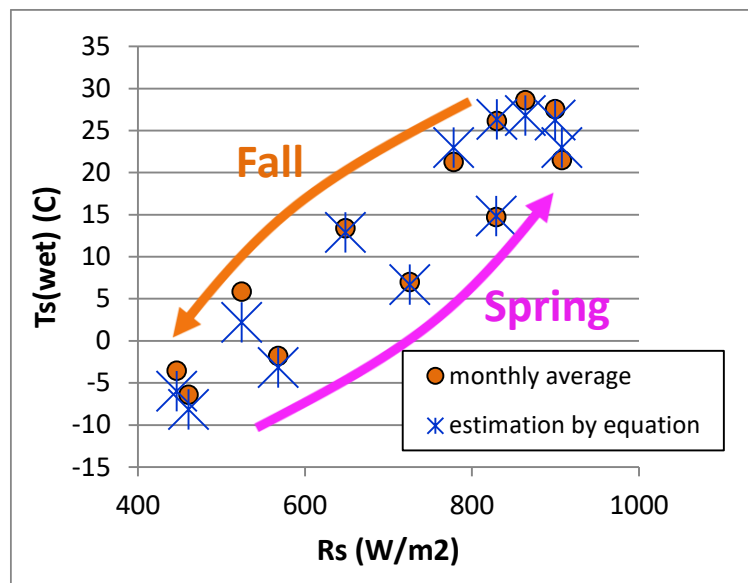


Figure 6. Monthly trend of R_s and $T_s(\text{wet})$ at 10:30 a.m. on clear-sky days along with estimated $T_s(\text{wet})$ from Equation 6.

The first component of Equation 6 “ $0.06R_s - 30.34$ ” is the average linear relationship between R_s and $T_s(\text{wet})$, as shown in Figure 5. The second component of the equation is the sine function describing the seasonal trend between R_s and $T_s(\text{wet})$ calibrated by the Shenmu data (Figure 6). The third component $f(\text{Lat})$ expresses the amplitude of the sine curve. At Shenmu (latitude = 38.78°), the amplitude of the sine curve was calibrated as 7.0. If the seasonal trend of the R_s vs $T_s(\text{wet})$ relationship is due to the thermal inertia of the Earth, the amplitude of the sine curve should change with latitude or with the difference of solar radiation that develops the seasons. The seasonal trend would be minimum at the equator and maximum at the location where the difference of solar radiation between summer and winter is largest.

Figure 7 shows the yearly trend of clear-sky solar radiation at 10:30 A.M. by latitude in the Northern Hemisphere. The seasonal difference of solar radiation is smallest near

the equator and largest at about 60° latitude. Assuming that the amplitude of the sine curve depends on the difference of solar radiation between summer and winter and assuming that the best value for amplitude at latitude = 38.78° (Shenmu) is 7.0, the amplitude of the sine curve was calibrated as shown in Figure 8.

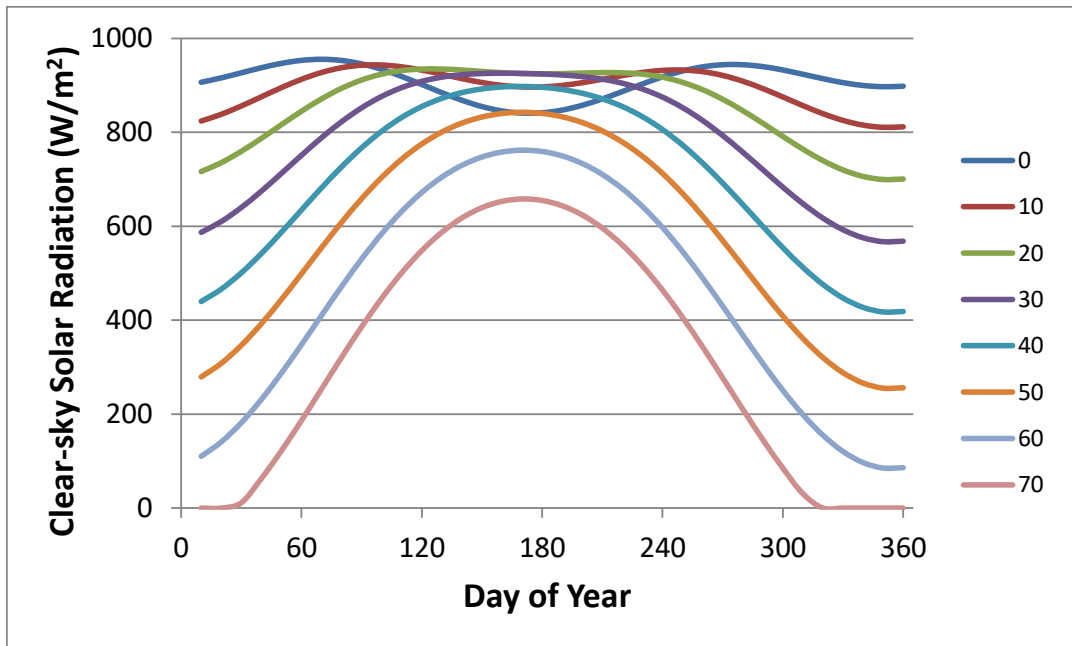


Figure 7. Yearly trend of clear-sky solar radiation at 10:30 A.M. by latitude from 0° to 70° in the Northern Hemisphere calculated assuming the atmospheric condition of the Shenmu measurement site.

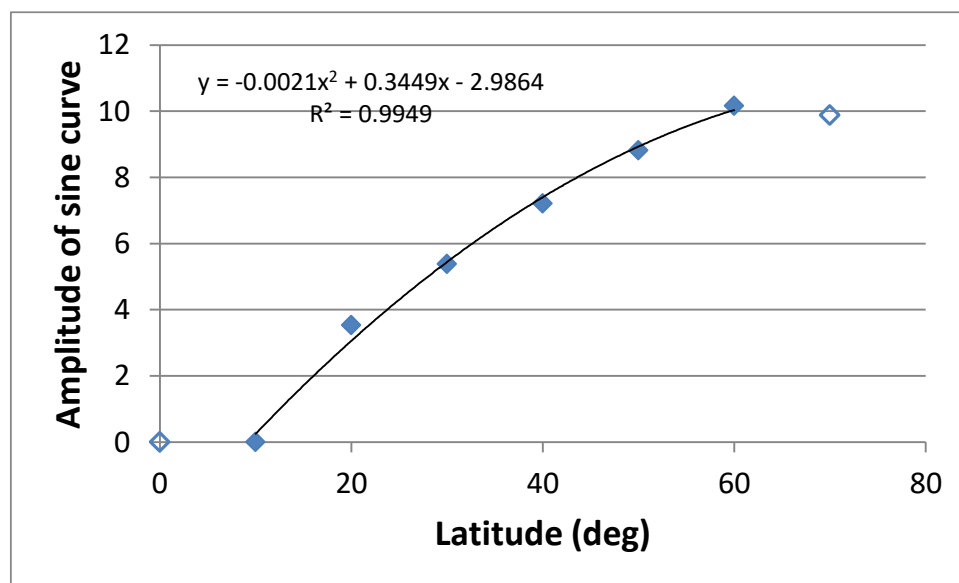


Figure 8. Calibration of the amplitude of the sine curve according to the difference of solar radiation between summer and winter. The amplitudes from 0-10° latitude were set as zero because of no clear winter at these latitudes.

The first version of the ATBD (ver. 1.0) contained an elevation function in Equation 8. However, it was eliminated in the previous ATBD (ver. 1.1) because an analysis indicated that the elevation function was inappropriate (Tasumi, 2013). This version of the ATBD temporarily follows the decision made for version 1.1 for impact of elevation. Future study is required to adequately represent the effect of elevation on $T_s(\text{wet})$ estimation.

The solar radiation used in Equation 6 is estimated using the solar zenith angle image of the satellite and the DEM. The following equations are based on the clear-sky solar radiation estimation procedure summarized in Allen et al. (1998), organized for application to ETindex estimation. Clear-sky solar radiation is calculated by

$$R_s = \tau \cdot R_a \quad (7)$$

where τ is atmospheric transmittance and R_a is extraterrestrial solar radiation (W m^{-2}).

Atmospheric transmittance is calculated as

$$\tau = 0.75 + 2 \times 10^{-5}z \quad (8)$$

where z is the elevation (m) given by the DEM. R_a can be calculated by the following equation:

$$R_a = \frac{G_{sc} \cdot \cos\theta}{d^2} \quad (9)$$

where G_{sc} is the solar constant of 1367 W m^{-2} , $\cos\theta$ is the cosine of the solar zenith angle, where the solar zenith angle is supplied as a part of the satellite image, and d is the relative distance between Earth and Sun calculated as

$$d = \sqrt{\frac{1}{1 + 0.033 \cdot \cos\left(\frac{2\pi}{365} \cdot DoY\right)}} \quad (10)$$

where DoY is day of year.

3-4. Ts(dry) Estimation

Compared to wet surface temperature ($T_s(\text{wet})$), dry surface temperature ($T_s(\text{dry})$) is much more sensitive to the micrometeorological condition over the surface (Kanda et al., 2010; Tasumi, 2011). Therefore, direct estimation of $T_s(\text{dry})$ without sufficient information of the micrometeorology over the surface might entail a considerable uncertainty in estimation accuracy. One operational solution to the problem is to estimate the difference between $T_s(\text{dry})$ and $T_s(\text{wet})$ (i.e., $T_s(\text{dry-wet})$), instead of direct estimation of $T_s(\text{dry})$. $T_s(\text{dry-wet})$ is expected to be more stable than $T_s(\text{dry})$ for changing micrometeorological condition. After estimating $T_s(\text{dry-wet})$, $T_s(\text{dry})$ is computed using the following equation:

$$T_s(\text{dry}) = T_s(\text{wet}) + T_s(\text{dry-wet}) \quad (11)$$

The relationship between R_s and $T_s(\text{dry-wet})$ at 10:30 A.M. for clear-sky days at Shenmu, China, is shown in Figure 9. The figure clearly shows the impact of wind speed on $T_s(\text{dry-wet})$. Within a similar wind speed condition, $T_s(\text{dry-wet})$ is linearly related to R_s . $T_s(\text{dry-wet})$ becomes smaller as wind speed becomes higher. No seasonal trend or effect of thermal inertia was found in the $T_s(\text{dry-wet})$ vs R_s relationship, probably because the seasonal impacts available in $T_s(\text{wet})$ and $T_s(\text{dry})$ are eliminated when the difference is taken.

The impact of wind speed on $T_s(\text{dry-wet})$ is explained by Figure 10. This figure shows the relationships between wind speed and the hypothetical surface temperatures for same season (May) for days having similar intensity of solar radiation ($900-950 \text{ W m}^{-2}$) at 10:30 A.M. for clear-sky days at Shenmu. The graph indicates that higher wind speed decreases the temperatures for both wet surface and dry surface, because wind promotes ET or sensible heat exchange. However, the decrement of surface temperature by wind speed is larger for dry surface than for wet surface, and this is the reason why $T_s(\text{dry-wet})$ becomes smaller as wind speed becomes higher.

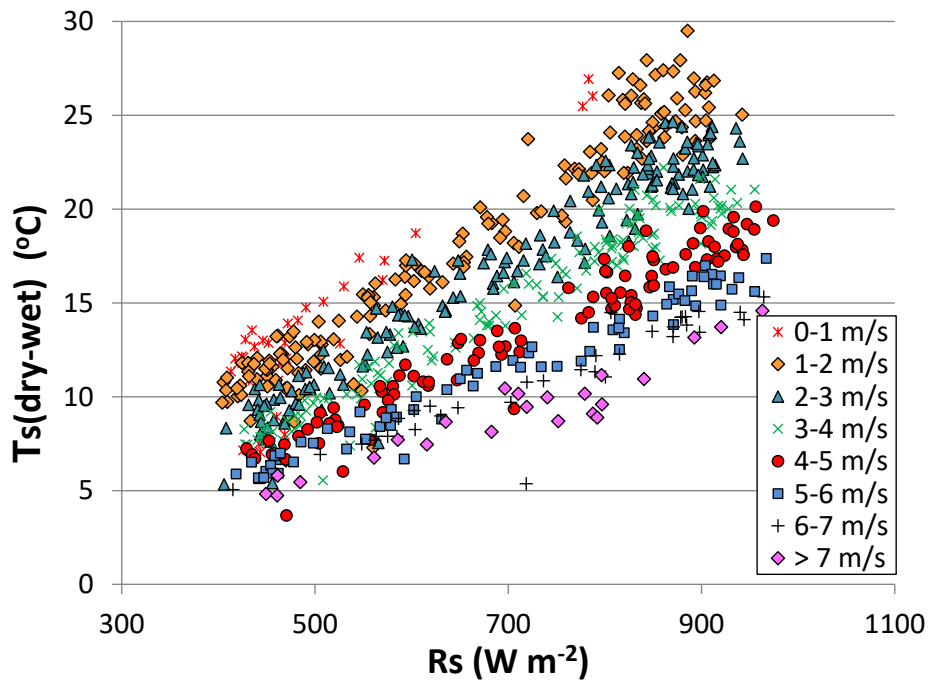


Figure 9. Relationship between measured solar radiation and estimated T_s (dry-wet) for eight wind speed groups at Shenmu, China, at about 10:30 A.M. (solar time) on clear-sky days during 2005–2008.

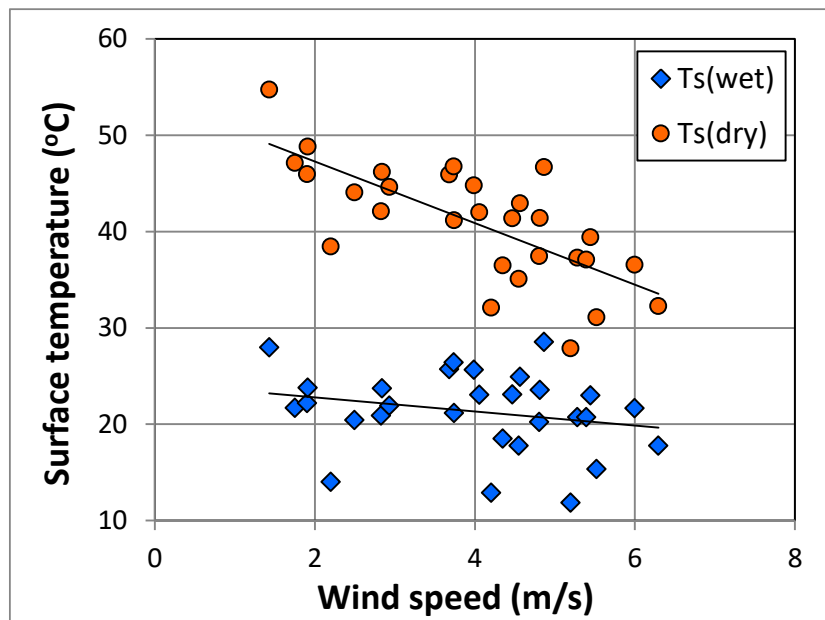


Figure 10. Relationships between wind speed and the hypothetical surface temperatures.

Considering the relations among $T_s(\text{dry-wet})$, R_s , and wind speed, we propose the $T_s(\text{dry-wet})$ estimation method summarized in Figure 11. Specifically, $T_s(\text{dry-wet})$ is proportional to R_s and the proportional factor changes with wind speed. The proportional factor was calibrated as shown in Figure 12, which uses the data shown in Figure 9. The slopes of the linear regression lines for the wind speed groups in Figure 9 were plotted with the average wind speed of each wind speed group. The resultant equation for $T_s(\text{dry-wet})$ estimation is the following:

$$T_s(\text{dry-wet}) = (-0.0023u + 0.0301)R_s \quad (T_s(\text{dry-wet}) \geq 0) \quad (12)$$

where $T_s(\text{dry-wet})$ is in $^{\circ}\text{C}$, u is wind speed at the height of 2 m in m s^{-1} , and R_s is solar radiation in W m^{-2} .

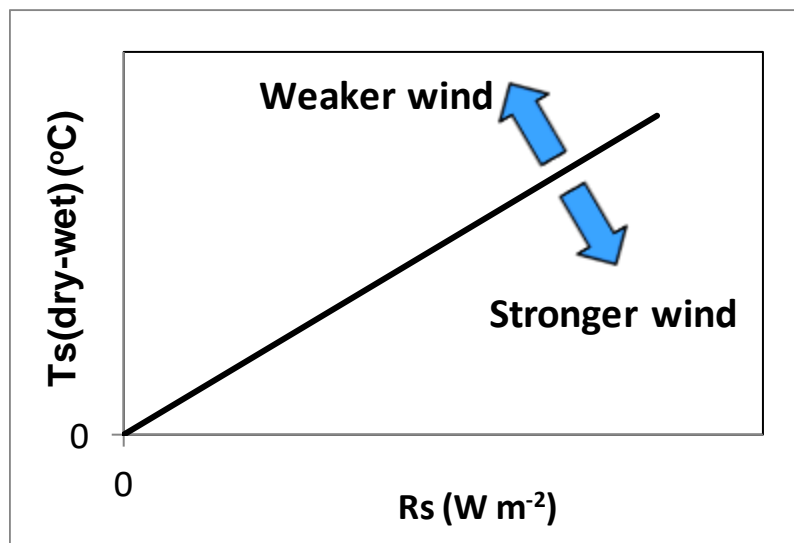


Figure 11. Proposed $T_s(\text{dry-wet})$ estimation method.

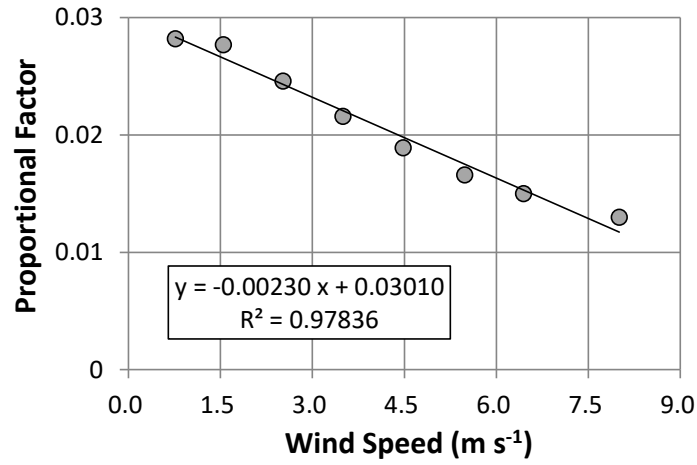


Figure 12. Calibration of the proportional factor.

Equation 12 applies when using wind speed at the height of 2 m. In the case in which the input wind speed data are for a different height, the wind speed data must be converted to wind speed at 2 m using the following equation:

$$u_2 = u_h \frac{\ln\left(\frac{2}{z_{om}}\right)}{\ln\left(\frac{h}{z_{om}}\right)} \quad (13)$$

where h is the height of the input wind speed data, u_h is wind speed at height h (m), and z_{om} is surface roughness for momentum transport (m).

The z_{om} is determined using the land cover/land use map. Recommended values of z_{om} for different land uses, shown in Table 1, were determined by considering the representative values summarized by Kondo (2000).

Table 1. Recommended z_{om} by land use type.

Land use	z_{om} (m)
Metropolitan	2
Forest	0.6
Town	0.3
Agriculture	0.05
Rangeland	0.05
Water/Snow	10^{-3}

3-5. Calibration for the Maximum Limit of ET_{index}

By definition, $ET_{index} = 1$ means that the surface has an ET value similar to the one from the hypothetical grassy reference field. The condition of such a surface is different from the “wet” surface determined for $T_s(wet)$. Usually, the reference field has positive sensible heat during the satellite overpass time, and therefore the ET_{index} of the wet surface exceeds 1.0. Namely, the adjustment factor, C_{adj} , of Equation 4 should exceed 1.0.

The C_{adj} of Equation 4 was calibrated using Shenmu data. Figure 13 shows a comparison of the latent heat flux from the “reference” surface defined by FAO and from the “wet” surface defined for our $T_s(wet)$ estimation. The result shows that the ET from the wet surface is 1.23 times greater than the ET from the reference surface if the relationship is assumed to be linear without intercept; however, a non-linear trend was found. The non-linearity indicates that C_{adj} depends on the intensity of the latent heat flux at the reference or the wet surface, which cannot be determined in this algorithm before determination of C_{adj} . Therefore, assuming a non-linear relationship, or assuming a linear relationship with intercept in Equation 13, is operationally difficult. In the current version of ATBD, we assume the C_{adj} of Equation 4 to be 1.23 by adopting a proportional assumption between the reference and the wet surface.

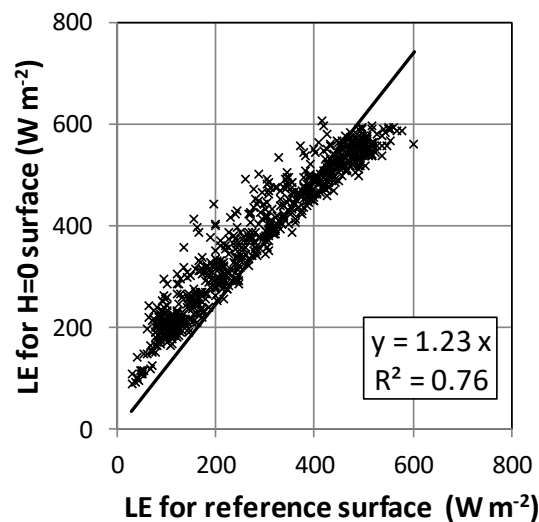


Figure 13. Comparison of latent heat flux from reference surface and from the “wet” surface at about 10:30 A.M. (solar time) for clear-sky days, Shenmu, China.

3-6. Adjustments and Filtering of ET_{index} Values on Daily Computation

ET_{index} expresses the efficiency of ET. It is also strongly related to the soil water content. ET_{index} = 0 means that there is no soil water to evapotranspire and that ET is thus zero. ET_{index} = 1.23 (i.e., maximum limit) means that sensible heat from the surface is zero at the satellite overpass time (e.g., 10:30 A.M.), which is the wettest condition that the satellite can identify via surface temperature. Thus, the most successful result would be that the calculated ET_{index} is between zero and 1.23, without any extra regulation.

However, there is no guarantee that the empirical equations employed in the GCOM-C ET_{index} algorithm are applicable to all regions and conditions. To improve the operational accuracy of ET_{index} estimation, we suggest additional regulations that might be applicable for the ET_{index}. Future studies for model improvement will be conducted to minimize this type of regulation by improving the ET_{index} estimation equations themselves.

Minimum and Maximum Values of ET_{index}

By the definition of dry surface, it is important to limit the minimum value of the ET_{index} to zero. The physical meaning of a negative ET_{index} is condensation of vapor, which is difficult at a dry surface during the satellite overpass time on clear-sky days. Therefore, a negative value of ET_{index} is most likely evidence of underestimation of ET_{index}. Additionally, it is effective to limit the maximum value of ET_{index} to 1.23, which represents the wet surface condition (H is zero). Theoretically, the actual ET_{index} can exceed the ET_{index} for the defined wet surface condition in some situations (e.g., in the case of the surface having negative sensible heat at 10:30 A.M. due to, for example, advection of sensible heat). However, setting a maximum number by accepting some underestimation in such rare conditions is a realistic strategy in this type of global application. A global application must target a very wide range of surface, subsurface, and climatic conditions. Also, the data processing should be fully automated. The empirical equations in the algorithm might work poorly in some specific conditions. Thus, setting these minimum and maximum limits of ET_{index} can help avoid the occurrence of large error. In this algorithm, ET_{index} is limited as

$$0 \leq ET\ Index \leq 1.23 \quad (14)$$

Additional Regulation for minimum value of ET_{index} by NDVI (Optional)

Figure 14 shows the relationship between NDVI and ET_{index} in an agricultural region of Urmia, Iran, for 6 Landsat satellite images during May to September, 2016. The selected six dates were “dry” images, where had no or little precipitation during the previous periods. ET_{index} dataset used in the analysis has been verified by Tasumi (2019). The spatial resolution was degraded to 270m for simulate GCOM-C, where, GCOM-C has 250m at-nadir resolution and typical operational resolution might be in the range of 250 to 300m (Tasumi et al., 2019). Because vegetation needs water to live, and because ET occurs when water is available, ET_{index} value is difficult to be in the gray-colored triangle region of the figure.

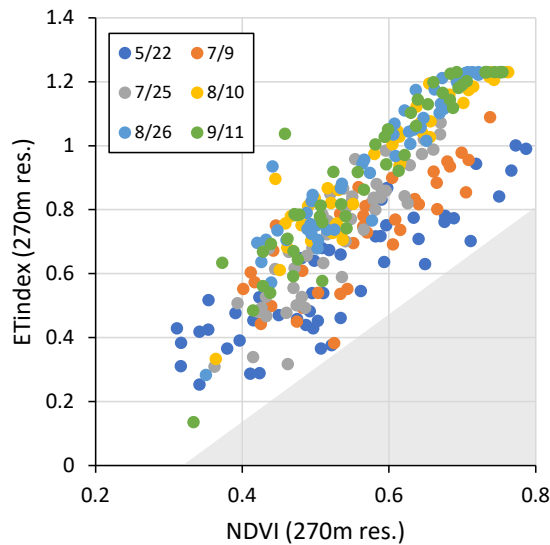


Figure 14. Relationship between NDVI and ET_{index} in an agricultural region of the Urmia, Iran, for 6 Landsat images during May to September, 2016.

The result of the analysis indicates that the following additional regulation may be applicable for improve the ET_{index} estimation accuracy;

$$ET\ Index(min) = 1.70 \times NDVI - 0.55 \quad (15)$$

Regulation of ET_{index} for Snow/Ice-covered Pixels and for No-sunlight Pixels

On snow/ice surfaces, most of the available energy is expected to be used for melting (i.e., consumed as latent heat of fusion or melting), and thus only a small portion of the available energy is spent on evaporation. Because detection of this very small latent heat is difficult with this type of empirical approach, an operationally reasonable method would be to assign zero ET_{index} for snow/ice surfaces. This limitation would not induce a large error, especially in the absolute value of ET, because the available energy itself is generally small on snow/ice surfaces, with their high surface reflectance and small gradient of absolute vapor pressure due to the cold air temperature.

Additionally, some locations on the Earth, typically within the north or south polar circles, may have no solar radiation at 10:30 A.M. This condition violates the application of some of the ET_{index} estimation equations. For such a surface, ET_{index} should be assigned as zero. Such a condition occurs in the winter season at high latitude, and the surface is likely to be covered by snow. Again, this limitation would not induce a large error, especially in the absolute value of ET, because the available energy itself is generally small on snow/ice surfaces, with their high surface reflectance and small gradient of absolute vapor pressure due to the cold air temperature.

3-7. ETindex Composite

16-day composite ETindex map is computed, simply by adopting the minimum ETindex value within each 16-day period (i.e. apply Minimum Value Composite). Taking the minimum value is to reject cloud contaminated pixels. Satellite-derived surface temperature, which is the primary input for the ETindex estimation, is very sensitive to cloud availability. Even tiny contamination of clouds can under-estimate surface temperature by 5 °C, and it can underestimate ETindex significantly.

3-8. Extra Adjustment of ETindex Values by Applying Soil Water Balance Model (Optional - Recommended)

The minimum value composite procedure described in the previous section is necessary to reject cloud-contaminated pixels. However, the process causes under-estimation of ETindex in some conditions. Applying soil water balance model is effective to improve estimation accuracy of ETindex. The soil water balance model is applied after ETindex is converted to ET. Following procedure is an example for monthly ET and ETindex estimation:

- (1) Compute ETindex for satellite observation dates.
- (2) Compute 16-day composite images of ETindex.
- (3) Compute daily ET (mm/day) using equation 16 with ET_0 computed by weather data. ETindex in the equation is the representative number (i.e. minimum value) of the 16-day, and ET_0 is daily values including cloudy days.

$$ET_{act} = ET_{index} \times ET_0 \quad (16)$$

- (4) Compute monthly ET (mm/month) by integrating daily ET derived by equation 16.
- (5) Compute soil evaporation of the month, using weather data and standard soil condition, adopting soil water balance model suggested by FAO (Allen et al., 1998).
- (6) If monthly ET computed by step (4) is less than evaporation derived by soil water balance (step (5)), over-write the ET value with the result of soil water balance model. The result is the monthly ET (mm/month) adjusted by soil water balance model.
- (7) Compute monthly ETindex using equation 1, with the output of step (6) and monthly ET_0 .

3-9. Calculation of Soil Moisture (Optional)

Estimating soil moisture requires information about soil water holding capacity. With this information, one can convert ETindex to soil moisture by adopting the SWEST method summarized in Tasumi and Kimura (2013).

The soil moisture estimation procedure has been tested for a natural grassland condition under semiarid climate using the weather and soil moisture observation data of Shenmu, China. The result indicated that soil moisture was sufficiently estimated at this location (Figure 15). The estimation error of the mean soil water content from zero to 25 cm depth was about 0.029 (i.e., estimation error of soil water was 2.9% of total volume of soil in 1 σ) on average for three years (Tasumi and Kimura, 2013).

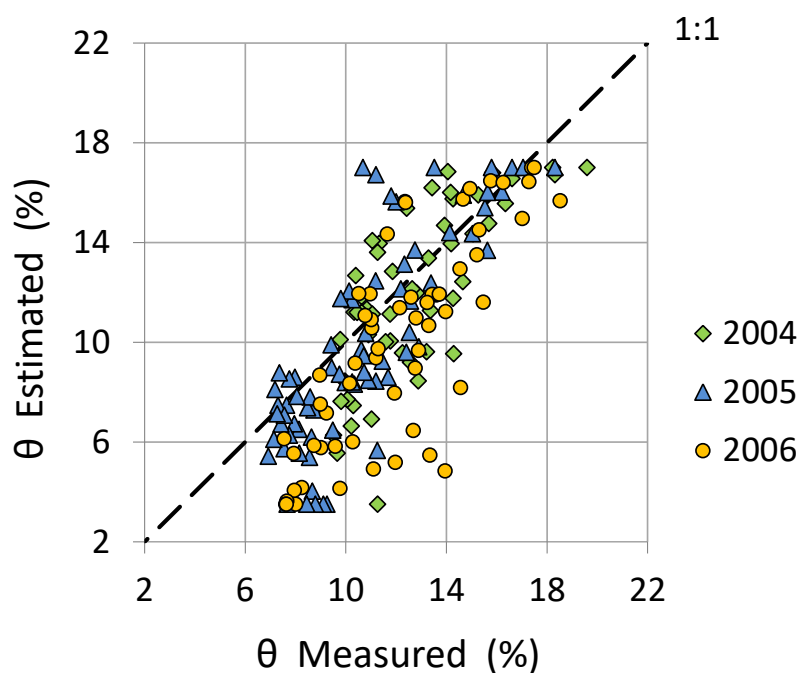


Figure 15. Performance of GCOM-C SM estimation model applied to Shenmu, China, during 2004-2006 (average soil moisture for root zone, 0-25 cm).

4. Application to Satellite Imagery and Information about Model Accuracy

Application tests and accuracy analyses have been made through the past years. Some of the results listed below were derived using the older version of the algorithm.

4.1. Global Application Test using MODIS Land Surface Temperature Product

The ET_{index} was estimated for the entire globe using the MODIS daily surface temperature map for the years 2001–2007 and daily global near-surface wind speed data for the corresponding years supplied by Dr. Mabuchi of Chiba University, Japan. The result of the annual average value for 2001 is shown in Figure 16. Using the daily information, daily ET_{index} maps were calculated. The daily maps contained effects of clouds and those had to be eliminated. In this application, the daily maps were grouped into series of 16 days, and the minimum pixel values of the 16-day series were picked up by assuming that the minimum values are the cloud-free, representative ET_{index} of the 16 days. For the pixels having no data during the 16 days, the ET_{index} value of 1.23 (i.e., the maximum value) was assigned by assuming that such pixels should be wet pixels (16 days of continuous clouds would likely bring some rainfall). No regulation using NDVI or land cover was applied in this application.

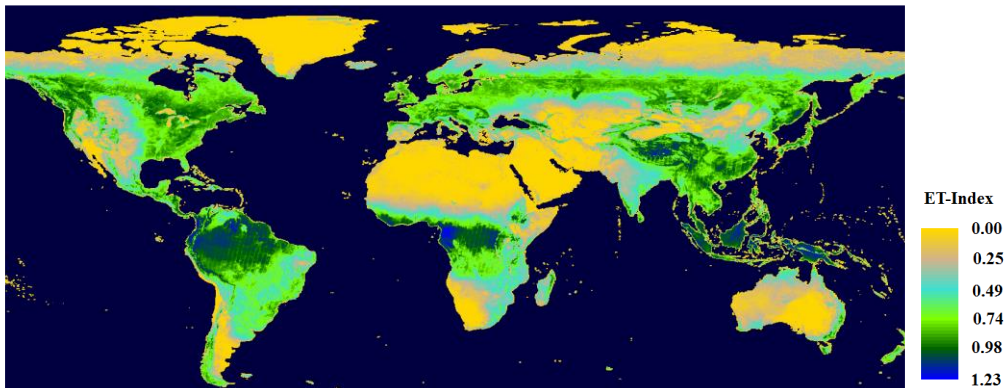


Figure 16. Estimated annual average ET_{index} for 2001 from ATBD ver. 1.2.

The 16-day ET_{index} was then converted to ET by using additional daily global meteorological data (air temperature, humidity, solar radiation) supplied by Dr. Mabuchi of Chiba University. The estimation result is shown in Figure 17. In this application, daily ET was calculated by the 16-day ET_{index} multiplied by the daily ET_0 , assuming that the ET_{index} is constant during the 16-day period. This assumption is

necessary to avoid the problem caused by cloud cover. Daily ET maps were then accumulated and the annual ET map shown in Figure 17 was derived.

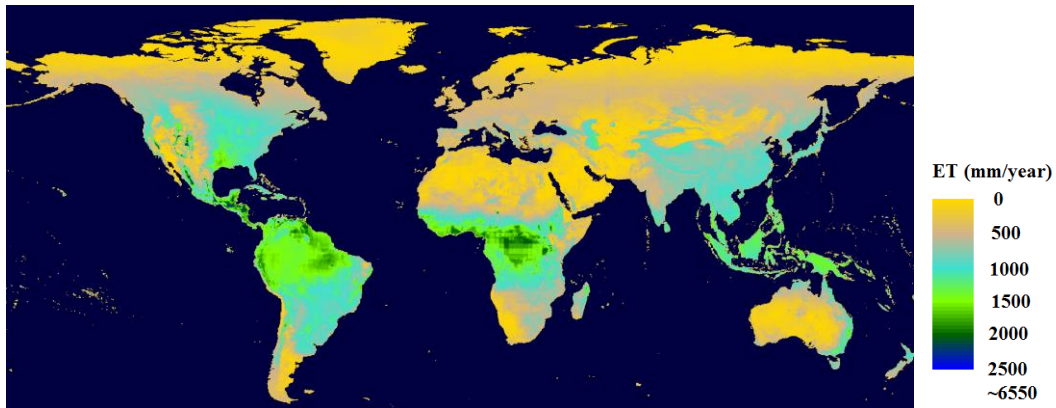


Figure 17. Estimated annual cumulative ET for 2001 from ATBD ver. 1.2.

Note that the annual averaged ETindex shown in Figure 16 is not a simple average of the 16-day ETindex maps. ETindex is calculated using annual ET and annual ETo. In the operational procedure, Figure 16 was derived after Figure 17 was derived. This application test confirmed that operational computation of the algorithm can be conducted without problem.

4.2. Regional Application Test using GCOM-C Land Surface Temperature Product

Regional application tests were made with GCOM-C Land Surface Temperature product version 1, for five locations in the world; Miyazaki and Tokyo (Japan), Southern Idaho (USA), Urmia (Iran), and Bangkok (Thailand). Figure 18 shows the result of ET estimation, with NDVI information. Estimated monthly ET showed reasonable values in Miyazaki, Tokyo, Southern Idaho and Urmia, except some mountainous regions, where further refinements of topographic adjustments are required. A malfunction of the estimation algorithm was found in Bangkok, Thailand, because the seasonal function of the current algorithm does not work for low-latitude area in monthly timescale. Further improvement of the model is required for the low latitudes.

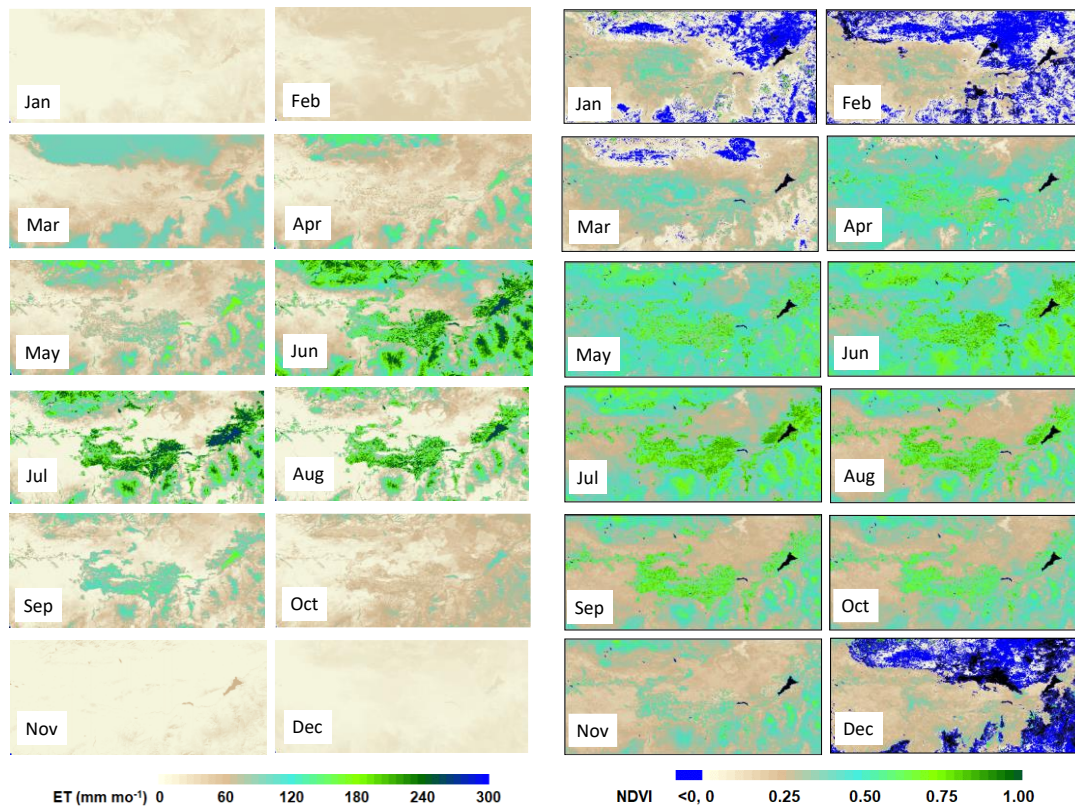


Figure 18. Estimated monthly ET for 2019 (left), and the monthly maximum NDVI (right), around Magic Valley irrigation area of Idaho, USA.

4.3. Analysis of ET_{index} for Model Applicability

The proposed ET_{index} estimation algorithm has a structure applicable to the entire globe. However, some of the most important equations are empirical equations developed by relying heavily on a location in China. One reasonable method to confirm the adequacy of the estimation algorithm is to calculate the ET_{index} value without applying the regulation suggested by Equation 14 and to evaluate the values in “wet” areas of the world. In “wet” areas, the ET_{index} is expected to be close to 1.23. If the estimated ET_{index} were far above 1.23, or far below 1.23, it would be an obvious indication that our ET_{index} estimation has a problem.

Figure 19 shows the seasonal trend of estimated ET_{index} for four selected “wet” areas of the world: central Africa, the eastern part of China, central South America, and Southeast Asia. These four “wet” areas were selected manually according to the result of the global application shown in Figure 16. The ET_{index} values of each area were averaged values of 20 sample pixels. Ideally, if the surface is in a wet-enough condition, ET_{index} reaches 1.23 (but does not exceed 1.23). The result shown in Figure 18 seems to sufficiently meet the criterion. This analysis indicates that the ET_{index} estimation is fairly functional, at least in these four selected regions.

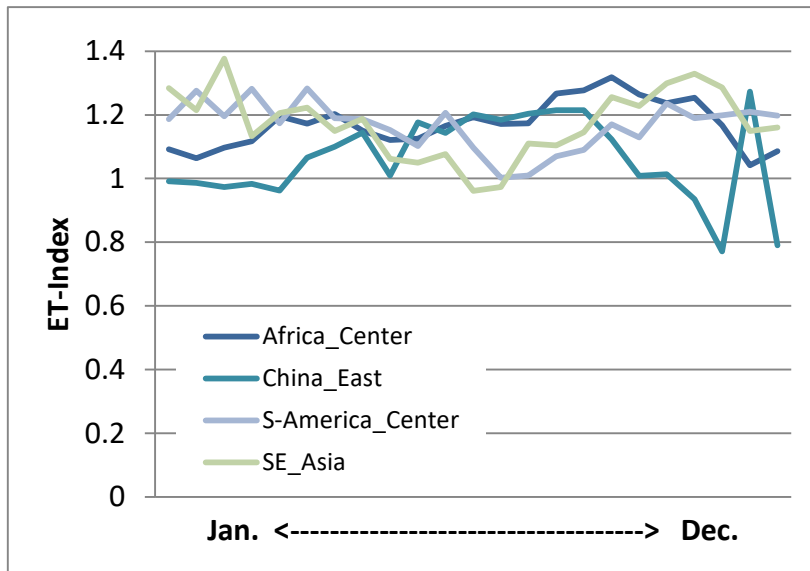


Figure 19. Seasonal trend of estimated ET_{index} for four “wet” regions in the world, 2001.

4.4. Reality Check of the Estimated Values using Outside Sources

ET and ET_{index} are closely related to other types of environmental information, such as climate condition, weather (such as rainfall), vegetation distribution, and so on. A reality check of the estimated ET_{index} was conducted using the following outside sources.

- (a) Global forest/non-forest map by JAXA (Figure 20)
- (b) Distribution of arid regions map by the Ministry of the Environment (Figure 21)
- (c) Estimated vegetation and precipitation maps of Africa by Sanga and Nonomura (2013) (Figure 22).

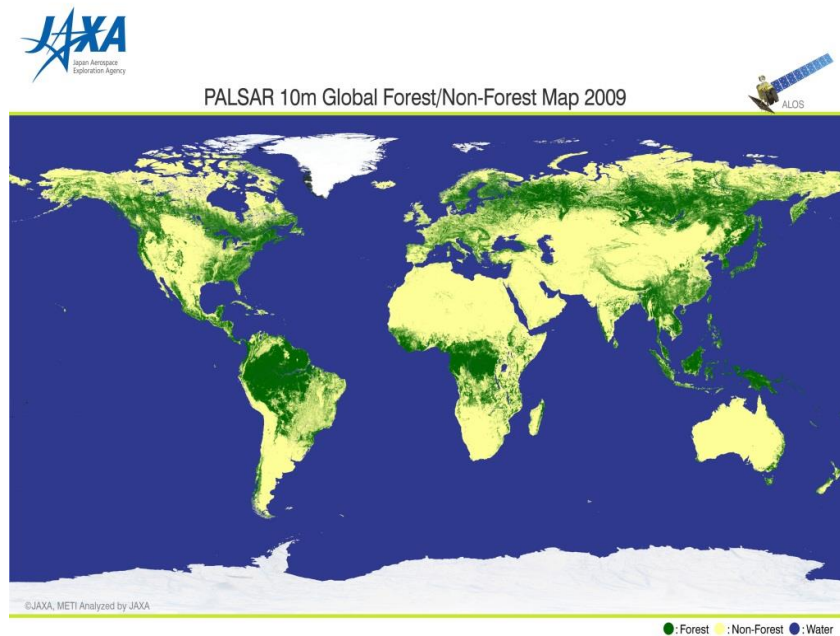


Figure 20. PALSAR 10-m global forest/non-forest map, 2009.

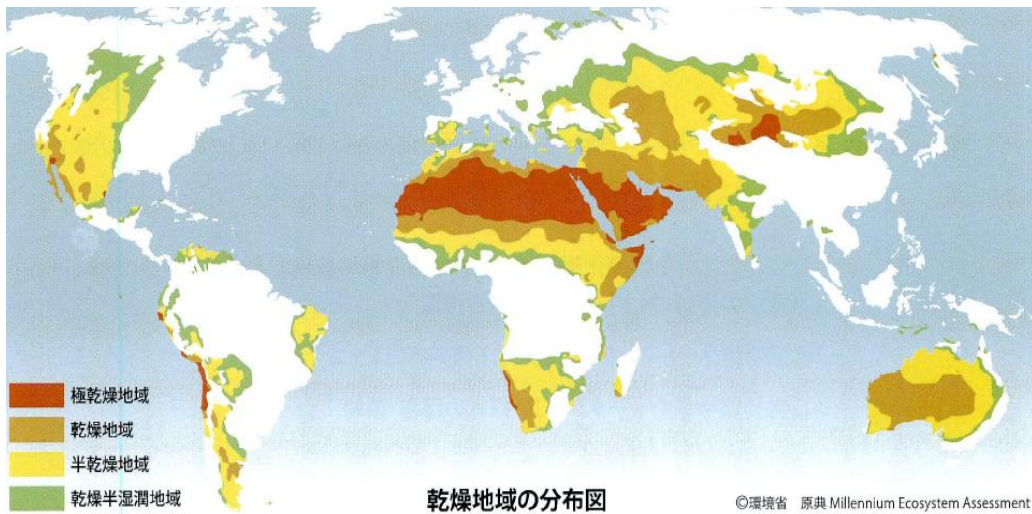


Figure 21. Distribution of arid regions by Ministry of the Environment, Japan.

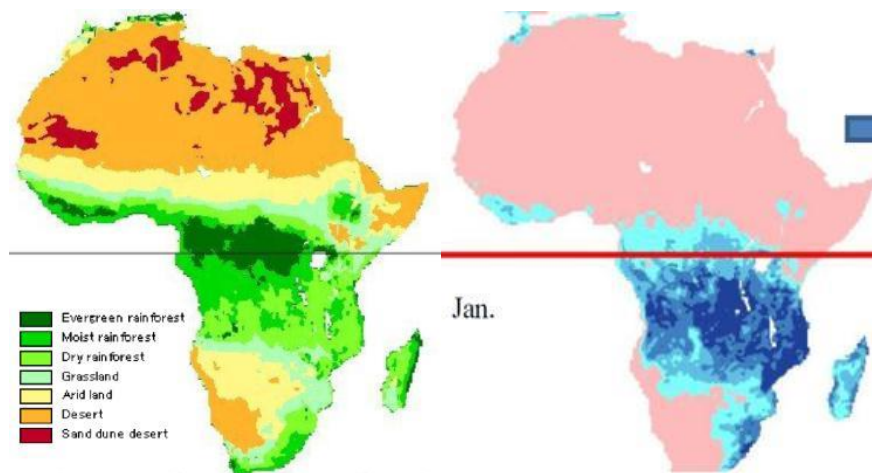


Figure 22. Estimated vegetation (left) and precipitation (right) maps of Africa.

These maps were compared with our estimated results shown in Figure 16. Note that the maps shown in Figures 20-22 are not for the year 2001 but are for different years or for multi-year general information.

The forest distribution (Figure 20) corresponded well with the high ET_{index} regions of Figure 16, and the distribution of arid regions (Figure 21) corresponded well with the low ET_{index} regions of Figure 16. The distribution of vegetation on the African continent (Figure 22, left) also corresponded well with the ET_{index} pattern in Figure 16. Additionally, the monthly precipitation distribution corresponded well with the 16-day estimated ET_{index} (Figure 23). The results of the comparison indirectly support the adequacy of the ET_{index} estimation algorithm.

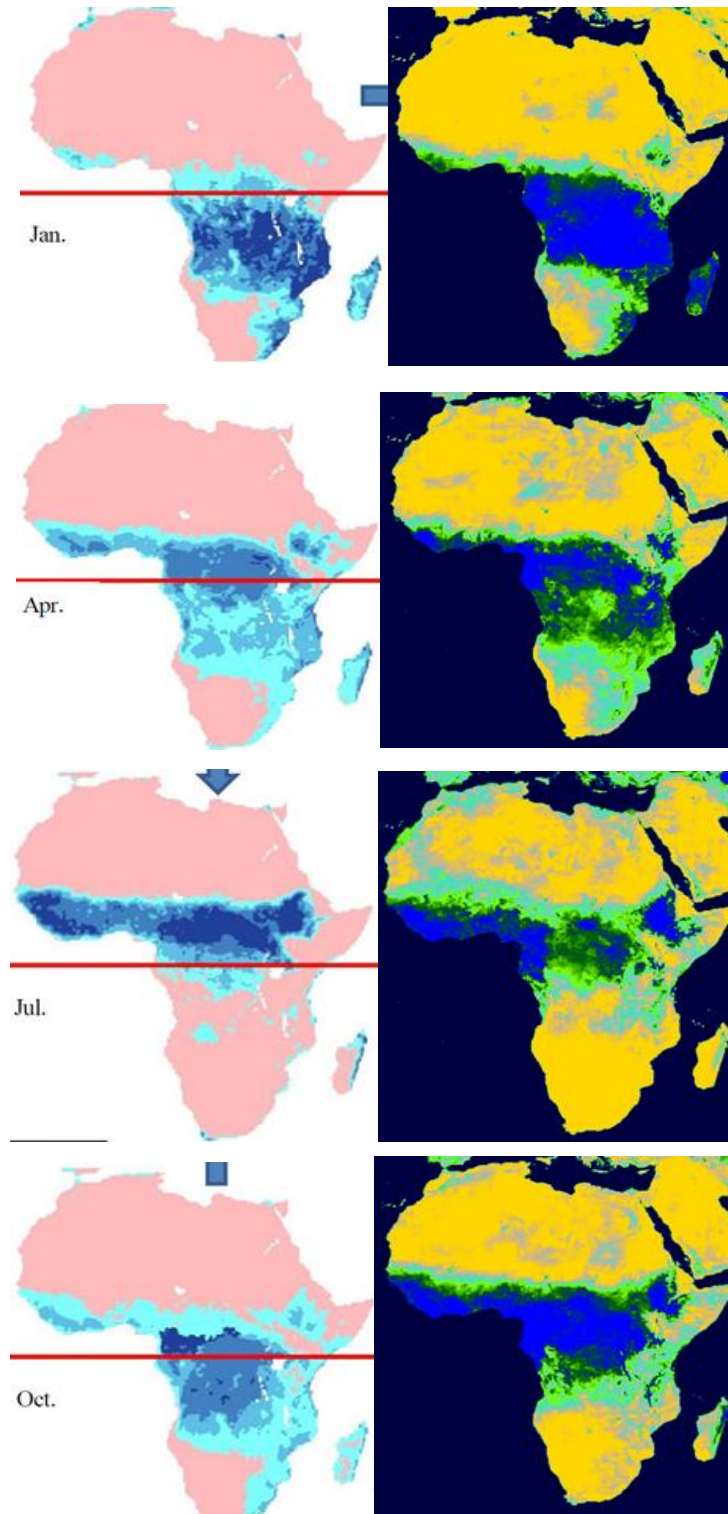


Figure 23. Precipitation distribution in Jan., Apr., Jul., and Oct. compared with corresponding 16-day ETindex maps.

Acknowledgements

This research was conducted under the Research Announcements for the Global Change Observation Mission (GCOM), funded by the Earth Observation Research Center, Japan Aerospace Exploration Agency (JAXA/EORC).

References

- Allen, R. G., Pereira, L. S., Raes, D., and Smith, M. (1998). "Crop Evapotranspiration." FAO Irrigation and Drainage Paper 56, Food and Agricultural Organization of the United Nations, Rome.
- Allen, R. G., Tasumi, M., Trezza, R., (2007). Satellite-based energy balance for mapping evapotranspiration with internalized calibration (METRIC)—model. *J. Irrig. Drain. Eng. ASCE*. 133.
- Bastiaanssen, W. G. M., M. Menenti, R. A. Feddes, A. A. M. Holtslag, (1998). A remote sensing surface energy balance algorithm for land (SEBAL): 1. Formulation. *J. of Hydr.* 212-213:198-212.
- Junsei K, (2000). *Atmospheric Science near the Ground Surface*. University of Tokyo Press. (in Japanese)
- Kanda, E., Tasumi, M., Ito, F., Ozaki, T., Kimura, R., (2010). 全球蒸発散量推定のための地表面温度指標についての基礎的研究. 2010 年度農業農村工学会講演要旨集.
- Kimura, R., (2007). Estimation of moisture availability over the Liudaogou River Basin of the Loess Plateau using new indices with surface temperature. *Journal of Arid Environments*, 70:237–252.
- Kogan, F. N. (1995). Application of vegetation index and brightness temperature for drought detection. *Adv. Space Res.*, 15, 91-100.
- Mabuchi, K. (2011). A numerical investigation of changes in energy and carbon cycle balance under vegetation transition due to deforestation in the Asian tropical region. *Journal of the Meteorological Society of Japan*, Vol. 89, No.1, pp.47-65.
- Mu, Q., Zhao, M., Running, S. W. 2011. Improvements to a MODIS global terrestrial evapotranspiration algorithm. *Remote Sensing of Environment*. 115:1781-1800.
- Sanga-Ngoie, K., Nonomura, A. 2013. Devising a framework for assessing renewable energy resources in the African biosphere using GIS and remote sensing techniques. 平成 24 年度日本リモートセンシング学会九州支部研究発表会論文要旨集 pp42-44.
- Senay, G. B., Budde, M., Verdin, J. P., Melesse, A. M. (2007). A coupled remote sensing and simplified surface energy balance approach to estimate actual evapotranspiration from irrigated fields. *Sensors*, 7:979-1000.
- Senay, G. B., Budde, M., Verdin, J. P. (2011). Enhancing the Simplified Surface Energy Balance (SSEB) approach for estimating landscape ET: Validation with the METRIC model. *Agricultural Water Management*, 98:606-618.

- Tasumi, M. and Kimura, R. (2013). Estimation of volumetric soil water content over the Liudaogou River Basin of the Loess Plateau using the SWEST method with spatial and temporal variability. *Agricultural Water Management*. 118:22-28.
- Tasumi, M. (2019). Estimating evapotranspiration using METRIC model and Landsat data for better understandings of regional hydrology in the western Urmia Lake Basin. *Agricultural Water Management*. 226:105805.
- Tasumi, M., Moriyama, M., and Shinohara, Y. (2019). Application of GCOM-C SGLI for agricultural water management via field evapotranspiration. *Paddy and Water Environment*. 17:75-82.

Appendix: Ts(wet) and Ts(dry) determination model for Shenmu weather measurement site

This model estimates surface temperatures for hypothetical wet and dry surfaces surrounded by a given weather condition. The wet surface is defined as the surface having no sensible heat, and the dry surface is defined as the surface having no ET. Hypothetical temperatures for the wet and the dry surfaces are named the wet surface temperature (Ts(wet)) and the dry surface temperature (Ts(dry)). The model estimates Ts(wet) and Ts(dry) using surface radiation and energy balance equations with observed ground-based weather data as input data.

Determination of Ts(dry) was made possible by using the energy balance model described below. However, direct determination of Ts(wet) was difficult because of the numerical instability of the iterative computation. To avoid this numerical instability, the surface temperature for a reference surface, Ts(ref), was employed as an initial intermediate parameter prior to estimating Ts(wet).

Calculation step 1 - determinations of Ts(ref) and Ts(dry)

This model derives Ts(ref) and Ts(dry) from surface energy balance computation. The energy balance equation is expressed as follows:

$$R_n = \ell E + G + H,$$

where R_n is net radiation ($W\ m^{-2}$), ℓE is latent heat flux ($W\ m^{-2}$), G is soil heat flux ($W\ m^{-2}$), and H is sensible heat flux ($W\ m^{-2}$).

Net radiation (R_n)

R_n is calculated from the radiation balance equation:

$$R_n = (1 - \alpha)R_s + L_{down} * \varepsilon - L_{up},$$

where R_s is measured solar radiation ($W\ m^{-2}$), α is measured albedo, L_{down} is measured incoming longwave radiation ($W\ m^{-2}$), L_{up} is outgoing longwave radiation ($W\ m^{-2}$) from

the hypothetical wet or dry surface, and ε is surface emissivity (= 0.98). L_{up} depends on $T_s(ref)$ and $T_s(dry)$.

Latent heat flux (ℓE) and soil heat flux (G)

ℓE for the wet surface is equivalent to E_{To} by definition. E_{To} is calculated by following the FAO56 equation for hourly data, using surface temperature instead of air temperature:

$$E_{To} = \frac{0.408\Delta(Rn - G) \cdot \frac{3600}{10^6} + \gamma \frac{37}{T_s(wet) + 273} u_2 (e_0 - e_a)}{\Delta + \gamma(1 + 0.34u_2)},$$

where Rn is net radiation ($W m^{-2}$), G is soil heat flux ($W m^{-2}$), $T_s(ref)$ is temperature of reference surface (C), Δ is saturation slope vapor pressure curve at T ($kPa C^{-1}$), γ is the psychrometric constant ($kPa C^{-1}$), e_0 is saturation vapor pressure at temperature T (kPa), e_a is actual vapor pressure (kPa), u_2 is wind speed ($m s^{-1}$), and the number $3600/10^6$ is for the conversion from $W m^{-2}$ to $MJ m^{-2} hr^{-1}$.

E_{To} ($mm hr^{-1}$) is converted to latent heat flux ($W m^{-2}$) as

$$\ell E = E_{To} * \ell * \frac{10^6}{3600},$$

where ℓ is latent heat of vaporization ($J kg^{-1}$) calculated as

$$\ell = 2.501 - 0.002361 * T_s(wet).$$

ℓE for the dry surface is zero by definition. G is calculated by the FAO equation as

$$\begin{aligned} G &= 0.1Rn && \text{(for daytime)} \\ G &= 0.5Rn && \text{(for nighttime)}. \end{aligned}$$

In this model, measured albedo is applied when calculating Rn , which slightly violates the definition of E_{To} (albedo = 0.23). The E_{To} used in this model is a value

adjusted by actual albedo of the site. Also, using measured vapor pressure in ETo estimation might overestimate ETo in the “wet condition” because the vapor pressure over the hypothetical wet surface might be higher than the measured value. This is a limitation of the model.

Sensible heat flux

Sensible heat flux is calculated by the bulk equation (Kondo, p. 142, Eq. 5.7-5.8):

$$H = C_p \cdot \rho \cdot C_H \cdot u_2 \cdot (T_s - T_a)$$

where C_p is the heat capacity of air ($J\ kg^{-1}\ K^{-1}$), ρ is the density of air ($kg\ m^{-3}$), T_s is the hypothetical surface temperature (i.e., $T_s(\text{ref})$ or $T_s(\text{dry})$) (C), T_a is the measured air temperature (C), and C_H is the bulk coefficient, which is calculated as

$$C_H = \frac{k^2}{\ln(z/z_0)\ln(z/z_T)}$$

where k is von Karman’s constant (0.41), z is the reference height (2 m), and z_0 and z_T are the surface roughness for momentum and heat transfer (m).

During the sensible heat flux computation, an air stability correction was applied via iteration using Monin-Obhukov similarity theory. In this model, measured air temperature was used to estimate H , which would generate an error on H estimation of the hypothetical wet and dry surfaces, as the air temperature over the hypothetical surfaces would be different from the measured air temperature. This is a limitation of the model.

Determination of $T_s(\text{wet})$ and $T_s(\text{dry})$

The optimal solutions for $T_s(\text{ref})$ and $T_s(\text{dry})$ are then found by the numerical iteration model. The optimal solutions are the values at which the following equations are valid.

$$(1 - \alpha)R_s + L_{down} \cdot \varepsilon - L_{up} = \ell E + G + H \quad (\text{for reference surface})$$

$$(1 - \alpha)R_s + L_{down} * \varepsilon - L_{up} = G + H \quad (\text{for dry surface})$$

Calculation step 2 - determination of Ts(wet)

Ts(wet) is calculated by adjusting Ts(ref) in proportion to the sensible heat:

$$Ts(wet) = Ts(ref) - \frac{Ts(dry) - Ts(ref)}{H(dry) - H(ref)} \times H(ref)$$

The equation is visualized in Figure App.1.

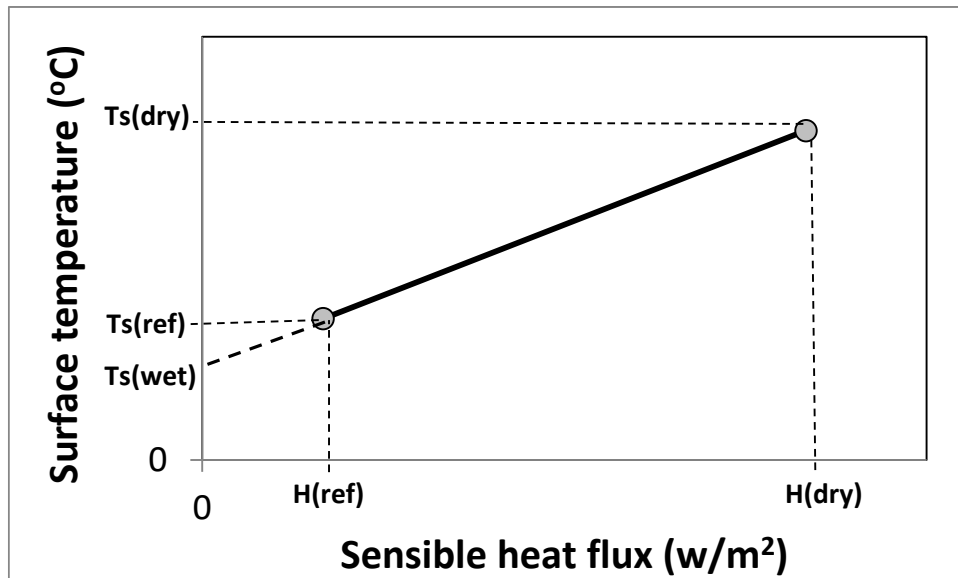


Figure App.1. Ts(wet) determination.